

- and G. R. Hall, *Phil. Mag.* **45**, 991 (1954); U. Ranon and K. Lee, *Phys. Rev.* **188**, 539 (1969).
- ³H. C. Meyer, P. F. McDonald, J. D. Stettler, and P. L. Donoho, *Phys. Letters* **24A**, 569 (1967).
- ⁴F. I. B. Williams, *Proc. Phys. Soc. (London)* **91**, 111 (1967).
- ⁵J. W. Culvahouse, D. P. Schinke, and D. S. Foster, *Phys. Rev. Letters* **18**, 117 (1967).
- ⁶J. Lewiner, P. H. E. Meijer, and J. K. Wigmore, *Phys. Rev.* **185**, 549 (1969).
- ⁷I. S. Ciccarello, R. Arzt, and K. Dransfeld **138A**, 934 (1965).
- ⁸W. Low, *Phys. Rev.* **101**, 1827 (1956).
- ⁹S. D. McLaughlan, *Phys. Rev.* **150**, 118 (1966).
- ¹⁰The term doublet is used here to denote the $|\Delta M_s| = 2$ transition within a ground triplet.
- ¹¹D. H. McMahon, *Phys. Rev.* **134**, A128 (1964).
- ¹²A. M. Stoneham, *Rev. Mod. Phys.* **41**, 82 (1969).
- ¹³C. M. Bowden and H. C. Meyer, *Phys. Status Solidi* **32**, K131 (1969).
- ¹⁴K. A. Mueller, *Phys. Rev.* **171**, 350 (1968).
- ¹⁵F. G. Fumi, *Acta Cryst.* **5**, 44 (1952).
- ¹⁶W. Voigt, *Lehrbuch der Kristallphysik* (Teubner, Leipzig, 1910).
- ¹⁷W. J. Dobrov, *Phys. Rev.* **146**, 268 (1966).
- ¹⁸P. F. McDonald, *Phys. Rev.* **177**, 447 (1969).
- ¹⁹N. Bloembergen, *Science* **133**, 1363 (1961).
- ²⁰J. S. Gradshteyn and J. M. Ryzhik, *Table of Integrals, Series and Products* (Academic Press, New York, 1965).
- ²¹C. M. Bowden, H. C. Meyer, P. F. McDonald, and J. D. Stettler, *J. Phys. Chem. Solids* **30**, 1535 (1969).
- ²²P. K. Wunsch, P. L. Donoho, H. C. Meyer, and C. M. Bowden, *Bull. Am. Phys. Soc.* **15**, 250 (1970).
- ²³S. Geschwind and J. P. Remeika, *Phys. Rev.* **122**, 757 (1961).
- ²⁴C. M. Bowden, H. C. Meyer, and P. L. Donoho, *Inter. J. Quantum Chem. Suppl.* (to be published).
- ²⁵R. Loudon, *Phys. Rev.* **119**, 919 (1960).
- ²⁶P. L. Donoho, P. K. Wunsch, P. F. McDonald, C. M. Bowden, and H. C. Meyer, *Bull. Am. Phys. Soc.* **15**, 250 (1970).
- ²⁷E. B. Royce and N. Bloembergen, *Phys. Rev.* **131**, 1912 (1963).

Effects of Uniaxial Stress on the Magnetic-Resonance Absorption Line Shapes for Non-Kramers Doublets

C. M. Bowden and H. C. Meyer

Solid State Physics Branch, Physical Sciences Laboratory, Redstone Arsenal, Alabama 35809

and

P. L. Donoho

Rice University, Houston, Texas 77001

(Received 18 June 1970)

A model is presented for uniaxial-stress-induced alterations in the intrinsically strain-broadened line shapes for magnetic-resonance absorption within a non-Kramers doublet for the point-group symmetries D_{3d} , C_{3v} , and O_h . (The term *doublet* is used here to denote the $|\Delta M_s| = 2$ transition within a ground triplet.) The uniaxial stress is introduced as boundary conditions in the model for the intrinsically strain-broadened line shapes for non-Kramers doublets given previously. The effects of uniaxial stress are considered for the EPR where the local site symmetry is O_h and D_{3d} . For the local symmetry C_{3v} , the effects of uniaxial stress are considered for the paraelectric resonance absorption. The model provides a means for evaluating the strength of the spin-lattice coupling from uniaxial-stress experiments, independent of the concentration of the paramagnetic impurity ions.

I. INTRODUCTION

Since the initial work done by Watkins and Feher,¹ much interest has been devoted to the determination of the parameters for the spin-lattice interaction for paramagnetic impurities in diamagnetic host lattices by introducing local crystal field perturbations using uniaxial stress. Feher's analysis² accounts reasonably well for first-order spectral shifts in the magnetic-resonance absorption for the Kramers ions Mn^{2+} and Fe^{3+} in MgO .

When the lowest-order nonzero contribution of

local crystal field perturbations is second order, as it is for transitions within a non-Kramers doublet,³ the spectral effect of uniaxial stress is quite different. Since the crystal field gives no first-order contributions to transitions within the doublet, the effect on the shape of the resonance line must be explicitly considered. In this paper we give a model for the effect of uniaxial stress on the shapes of intrinsically strain-broadened magnetic-resonance line shapes for transitions within a non-Kramers doublet.^{3a} The model is given for the EPR for the local site symmetries O_h and D_{3d} . The case of C_{3v}

without inversion symmetry is treated for the paraelectric resonance (PER), since the electric dipole transitions occur in first order, whereas the corresponding magnetic quadrupole transitions occur in second order.⁴ In each of the cases of local site symmetry, the spin-lattice coupling coefficients are treated as adjustable parameters, and thus must be determined from a comparison of the model with the appropriate uniaxial-stress experiments. The model thus gives a means for evaluating the spin-lattice parameters for non-Kramers ions independent of the concentration of the paramagnetic impurity ion.

II. THEORY

We introduce uniaxial stress as boundary conditions in the model for the intrinsically strain-broadened line shapes presented earlier.⁵ The absorption intensity is therefore that given in Ref. 5, i. e.,

$$I(E) = \int_{-\infty}^{\infty} |\langle i | H_{\text{rf}} | f \rangle|^2 G(E - E') \prod_i p_i(e_i) de_i, \quad (1)$$

$i = 1, \dots, 6.$

Here $G(E)$ is the homogeneous distribution, the width of which is determined by the lifetime broadening and E is the energy of separation between the states of the doublet. The first term in the integral in (1) is the square of the matrix element of the rf field which couples the states of the doublet, and the $p_i(e_i)$ are the probability distributions in the local strain amplitudes e_i . The term E' is the correction in the transition energy caused by the local crystal field perturbations, i. e., $E' = E'(e_1, \dots, e_6)$. Following the procedure of Ref. 5, we assume that the local strain amplitudes follow a random distribution in the crystal lattice, so we take the probability distributions $p_i(e_i)$ as Gaussian. The introduction of uniaxial stress occurs as a boundary condition with regard to the probability distributions. These distributions are then given by

$$p_i(e_i) = (\lambda_i/\pi^{1/2}) \exp[-\lambda_i^2(e_i - e_i^0)^2], \quad (2)$$

where e_i^0 is the component of the local strain e_i induced by the application of uniaxial stress.

A. Site Symmetry D_{3d} and C_{3v} : Magnetic Quadrupole and Phonon-Induced Transitions

In the absence of hyperfine interaction the magnetic resonance experiments can be interpreted on the basis of an effective spin-1 formalism.^{3,6} The inhomogeneous strain broadening of the line shape depends upon the crystal field perturbation term \mathcal{H}_p in the spin Hamiltonian,⁵

$$\mathcal{H}_p = S \cdot \tau \cdot S, \quad (3)$$

where the elements of the tensor τ are linearly proportional to the local strain components,^{3,5} and the coefficients are the appropriate spin-lattice coupling

parameters.² From the eigenvalues of the Hamiltonian for the spin-1 formalism, the resonance frequency ν is given by the expression

$$h\nu = 2g_{\parallel}\beta H_z + 8\Delta^2/h\nu_0, \quad (4)$$

to second order. Here, H_z is the axial component of the magnetic field, $h\nu_0$ is the unperturbed Zeeman splitting, and Δ is a distribution in the strain amplitudes which mixes only the states of the doublet within the triplet manifold defined by the Hamiltonian,⁵ i. e.,

$$\Delta = \frac{1}{4} [(\tau_{11} - \tau_{22}) - 2i\tau_{12}]. \quad (5)$$

As was done previously,⁵ (5) can be written in the form

$$\Delta = \frac{1}{2} (\frac{1}{2} \tau_0 - i\tau_6), \quad (6)$$

where

$$\tau_0 = \tau_{11} - \tau_{22} = (G_{11} - G_{12})(e_1 - e_2) + 2G_{14}e_4 \quad (7)$$

and

$$\tau_6 = \tau_{12} = G_{14}e_5 + \frac{1}{2}(G_{11} - G_{12})e_6. \quad (8)$$

Here, the G_{ij} are the spin-lattice coupling coefficients and the e_k are the strain amplitudes in the Voigt⁷ notation. From (7) and (8) it is seen that τ_0 and τ_6 are completely independent. It has been shown that (1) may be reduced from an integral over a six-dimensional volume defined by the six independent strain components to one over a two-dimensional volume defined by τ_0 and τ_6 .⁵ Using (2), the probability distributions in τ_0 and τ_6 from Eqs. (16) and (17) of Ref. 5 become

$$P_0(\tau_0) = (\gamma_0/\pi)^{1/2} \exp[-\gamma_0(\tau_0 - \tau_0^0)^2] \quad (9)$$

and

$$P_6(\tau_6) = (\gamma_6/\pi)^{1/2} \exp[-\gamma_6(\tau_6 - \tau_6^0)^2], \quad (10)$$

respectively. Here, τ_0^0 and τ_6^0 correspond to the local strains induced by applied stress, i. e., if we let

$$a_1 = G_{14}, \quad a_2 = G_{11} - G_{12}, \quad (11)$$

we have

$$\tau_0^0 = a_2(e_1^0 - e_2^0) + 2a_1e_4^0 \quad (12)$$

and

$$\tau_6^0 = a_1e_5^0 + \frac{1}{2}a_2e_6^0. \quad (13)$$

We also have in this case the equivalence relation between the distribution parameters⁵ γ_0 and γ_6 , i. e.,

$$\gamma_6 = 4\gamma_0 = \gamma. \quad (14)$$

We take the homogeneous distribution $G(E)$ as a Gaussian,⁵

$$G(E - E') = (\sigma/\pi^{1/2}) \exp[-\sigma^2[E - \alpha(\frac{1}{4}\tau_0^2 + \tau_6^2)]^2], \quad (15)$$

and note that the square of the matrix element for the rf field for EPR is to second order,⁵

$$|\langle i | \mathcal{K}_{\text{rf}} | f \rangle|^2 = 4g_{\parallel}^2 \beta^2 \alpha^2 H_z^2(t) \Delta^2. \quad (16)$$

Here, $H_z(t)$ is the z component of the rf magnetic field and

$$\alpha = 2/h\nu_0 \quad (17)$$

is the unperturbed Zeeman splitting factor and Δ is given by (6). Using (9), (10), (15), and (16), and using the computational scheme of Ref. 5, Eq. (1) for the absorption becomes

$$I(E) = (4 \mathcal{K} \gamma \sigma / \pi^{3/2}) e^{-\gamma r_0^2} e^{-\sigma^2 E^2} \int_0^{2\pi} \int_0^{\infty} dr d\theta r^3 \times \exp[-ar^4 - cr^2 + \Phi(\theta)r]. \quad (18)$$

Here, we have

$$r_0^2 = \frac{1}{4} (\tau_0^0)^2 + (\tau_6^0)^2, \quad (19)$$

$$a = \sigma^2 \alpha^2, \quad c = \gamma - 2\alpha \sigma^2 E, \quad (20)$$

and

$$\Phi = \tau_0^0 \cos \theta + 2\tau_6^0 \sin \theta. \quad (21)$$

The constant \mathcal{K} in (18) is

$$\mathcal{K} = 4 g_{\parallel}^2 \beta^2 H_z^2(t) / (h\nu_0)^2. \quad (22)$$

The integration over θ results in the expression

$$I(E) = (2 \mathcal{K} \gamma \sigma / \pi^{1/2}) e^{-\gamma r_0^2} e^{-\sigma^2 E^2} \int_0^{\infty} dr r^3 \times J_0(2\gamma r_0 r) \exp(-ar^4 - cr^2), \quad (23)$$

where $J_0(Z)$ is the modified Bessel function in the argument of order zero. If we make the substitution $Z = 2\gamma r_0 r$ and integrate, (23) becomes

$$I(E) = \mathcal{K} \gamma / (\pi^{3/2}) \sigma \alpha^2 e^{-\gamma r_0^2} e^{-\sigma^2 E^2} e^{c^2/8a} \times \sum_{n=1}^{\infty} \frac{n(2\lambda)^{-(n-1)/2}}{2^{2(n-1)} (n-1)!} D(u)_{-(n+1)}, \quad (24)$$

where

$$\lambda = a / (16\gamma^4 r_0^4) \quad (25)$$

and

$$u = c / \sqrt{2a}. \quad (26)$$

The terms $D(u)_{-\nu}$ in the series in (24) are the parabolic cylinder functions of order ν . In Fig. 1 is shown the derivative of the absorption distribution obtained from (24) as a function of applied uniaxial strain for a particular set of values for the intrinsic parameters and the spin-lattice coefficients.

B. Site Symmetry C_{3v} : Electric Dipole Transitions

In this case we consider that the paramagnetic-ion-impurity site lacks inversion symmetry. Thus, the initial wave functions for the states of the doublet have both even and odd parity components, so that an electric field \mathcal{E} can have a first-order ef-

fect.⁸ In a region of a microwave cavity where $H_{\text{rf}} = 0$, where H_{rf} is the magnetic field component of the radiation field, the square of the matrix element coupling the states is^{5,9}

$$|\langle i | \mathcal{J}_{\text{rf}} | f \rangle|^2 = \mathcal{E}^2(t) R^2 (1 - 2\alpha^2 \Delta^2) \quad (27)$$

through second-order terms in the crystal field perturbation. Here R is the spin-electric-field coupling,⁵ α is given by (17), and Δ is the distribution in the local strain amplitudes given by (6)–(8). The factor $\mathcal{E}(t)$ in (27) is the component of the electric rf field normal to the symmetry axis.

We assume that there are no large stationary electric fields present. Thus, the stationary effective spin Hamiltonian is the same as for the previous case and the resonance frequency is given by (4). We again invoke the uniaxial-stress boundary conditions given in (9) and (10) and use (15) and (27) in (1) to obtain the expression for the resonance absorption as a function of applied stress. The procedure for the calculation is the same as in the previous case, and the result is

$$I(E) = \frac{2 \mathcal{K}' \sigma \gamma}{\pi^{(1/2)}} e^{-\gamma r_0^2} e^{-\sigma^2 E^2} \left\{ \frac{\pi^{(1/2)}}{2\sigma\alpha} e^{c^2/4a} \right.$$

EPR ABSORPTION DERIVATIVE FOR D_{3d} LOCAL SITE SYMMETRY-UNIAXIAL STRESS

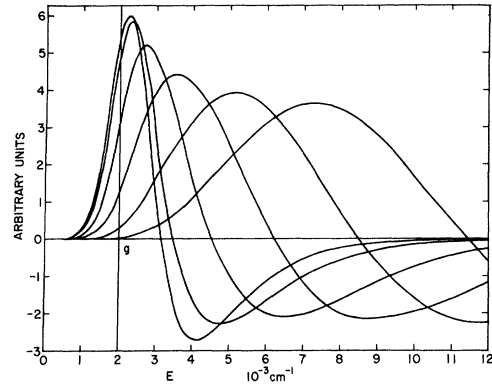


FIG. 1. EPR-absorption derivative for D_{3d} site symmetry for various values of the applied uniaxial strain. The elastic constants used are those given by Huntington (see Ref. 11) for CaF_2 and the spin-lattice coefficients used are those given by McDonald [P. F. McDonald, Phys. Rev. **177**, 447 (1969)] for $\text{CaF}_2: \text{U}^{4+}$. The applied strain is taken along the [111] with site axis along the $[1\bar{1}\bar{1}]$. The amplitude of the first lobe of the derivative decreases with increased applied strain, the values of which are successively 0, 0.5, 1.5, 2.0, 2.5, and 3.0 in units of 10^{-4} . The homogeneous distribution parameter is taken to be $\sigma^{-1} = 0.667 \times 10^{-3} \text{ cm}^{-1}$ and the intrinsic strain distribution parameter is taken as $\alpha\gamma^{-1} = 9.946 \times 10^{-3} \text{ cm}^{-1}$. The position of the "g value" for the absorption distributions, i. e., the position of the peak of the undisplaced homogeneous distribution is indicated in the figure by the vertical line.

$$\times \left[1 - \Phi \left(\frac{c}{2\sqrt{a}} \right) \right] + e^{c^2/8a} \sum_{n=1}^{\infty} \frac{\lambda^{2n}}{2^{(5n+1)/2} a^{(n+1)/2} n!} \\ \times \left[1 - 2 \left(\frac{\alpha n}{\lambda} \right)^2 \right] D_{-(n+1)} \left(\frac{c}{\sqrt{2a}} \right) \Bigg\}, \quad (28)$$

where

$$\mathcal{K}' = \mathcal{E}^2(t) R^2. \quad (29)$$

As before, the terms $D_{-\nu}(u)$ in (28) are the parabolic cylinder functions of order ν , and the term $\Phi(z)$ is the error function in the argument z . The derivative of (28) is shown in Fig. 2 as a function of applied uniaxial strain. For comparison, the values for the intrinsic parameters and the spin-lattice coefficients are the same as those used for Fig. 1.

C. Site Symmetry O_h : Magnetic Quadrupole and Phonon-Induced Transitions

The form of the spin Hamiltonian is again for the spin-1 formalism but with octahedral symmetry with a perturbation to lower symmetry caused by crystal defects. Thus, the spin Hamiltonian \mathcal{H} is of the form

$$\mathcal{H} = \beta \vec{S} \cdot \vec{g} \cdot \vec{H} + \vec{S} \cdot \vec{D} \cdot \vec{S}. \quad (30)$$

The last term is used to describe local crystal field perturbations, and thus the elements of the coupling tensor D can be written as a linear combination of the local strain components. We consider only the transitions within the non-Kramers doublet, i. e.,

$|\Delta M_s| = 2$, and thus the resonance frequency is obtained from the eigenvalues of (30) and is,⁵ to second order,

$$h\nu = 2g\beta H_0 + (8/h\nu_0) (\Delta^2 + \Delta'^2). \quad (31)$$

Here, $h\nu_0 = 2g\beta H_0$ is the unperturbed Zeeman splitting and

$$\Delta = \frac{1}{4} (D_{11} - D_{22} - 2i D_{12}) \quad (32)$$

and

$$\Delta' = \frac{1}{2} (D_{13} - i D_{23}). \quad (33)$$

From (31), the correction E' to the resonance frequency which arises from the crystal field perturbations is given explicitly in terms of the local strain components⁵:

$$E' = \alpha' [a(e_{11} - e_{22})^2 + 4b(e_{12}^2 + e_{31}^2 + e_{23}^2)], \quad (34)$$

where

$$\alpha' = (h\nu_0)^{-1}, \quad a = \frac{9}{8} G_{11}^2, \quad b = \frac{1}{2} G_{44}^2, \quad (35)$$

and G_{11} and G_{44} are the independent spin-lattice coupling coefficients. The strain amplitudes in (34) are referred to the crystal axes.

As pointed out in Ref. 5, the distribution functions Δ and Δ' couple the states of the doublet and the singlet into the states of the doublet, respectively. Therefore, the transition probability for transitions within the doublet will be quite different depending on whether the rf magnetic field is parallel or perpendicular to the dc magnetic field H_0 . We assume that the local strains follow a random distribution, and thus take the probability distribution for each strain amplitude to be Gaussian. The uniaxial stress is again introduced as boundary conditions in the model, so that the probability distributions take the form (2). For the same reasons given in Ref. 5, we take the homogeneous distribution, $G(E)$ in (1), as a δ function. We treat the two cases for the magnetic field orientation separately:

Case A: $\vec{H}_{\text{rf}} \perp \vec{H}_0$.

The matrix element for the rf field is, to first order in the spin functions,

$$|\langle i | \mathcal{H}_{\text{rf}} | f \rangle|^2 = [2 G_{44}^2 H_{\text{rf}}^2 / (h\nu_0)^2] (e_5^2 + e_4^2), \quad (36)$$

where the strain amplitudes have been written in the Voigt notation.⁷ We let

$$K = \frac{4 H_{\text{rf}}^2 \lambda_1^2 \lambda_2^2}{\alpha (2\pi^2 ab^3)^{1/2}} \quad (37)$$

and make the cubic approximation that the diagonal intrinsic strain distributions are all equal with the mean square value proportional to λ_1^{-2} ; and likewise, the off-diagonal ones are equal with the mean square value proportional to λ_2^{-2} . Then, using (2), (34), and (36) in (1) and using the method for taking the necessary integrals given in Ref. 5, we obtain

PER ABSORPTION DERIVATIVE FOR C_{3v} LOCAL SITE SYMMETRY-UNIAXIAL STRESS

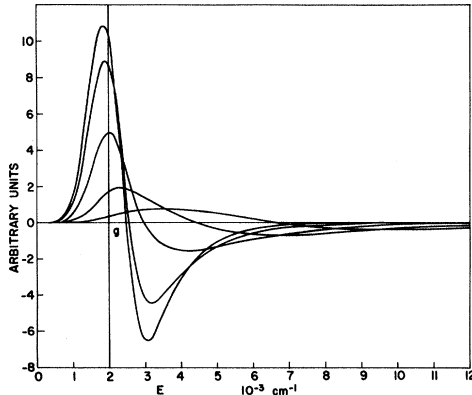


FIG. 2. PER-absorption derivative for C_{3v} site symmetry. The values used for the intrinsic parameters as well as the direction of the applied strain and orientation of the site axis are the same as those used for Fig. 1. The amplitude of the first lobe of the derivative decreases with increased applied strain, the values of which are successively 0, 0.5, 1.5, 2.0, and 2.5 in units of 10^{-4} . The position of the g value for the absorption distributions, i. e., the position of the peak of the undisplaced homogeneous distribution, is indicated in the figure by the vertical line.

the expression for the absorption intensity

$$I(E) = K e^{-(\lambda_1^2/2)u_0^2} e^{-(\lambda_2^2/4)\alpha'b} r_0^2 e^{-(\lambda_2^2/4\alpha'b)E} \\ \times \int_0^E d\tau \frac{(E-\tau)^{3/2}}{\tau^{1/2}} e^{-(\lambda_1^2/2\alpha'a)\tau} \\ \times \exp\left(\frac{\lambda_2^2}{4\alpha'b} [\tau + 2r_0 (\alpha'b)^{1/2} (E-\tau)^{1/2}]\right) \\ \times \cosh\left[\lambda_1^2 u_0 \left(\frac{\tau}{\alpha'a}\right)^{1/2}\right]. \quad (38)$$

Here, we have written

$$u_0 = e_1^0 - e_2^0, \quad (39)$$

$$r_0 = [(e_4^0)^2 + (e_5^0)^2 + (e_6^0)^2]^{1/2}, \quad (40)$$

and a , b , and α' are defined by (35). As before, the e_i^0 are the local strain amplitudes induced by applied stress.

In order to simplify the integral in (38), we consider two cases for the applied stress.

1. Applied Uniaxial Stress along the [100]

In this case,

$$r_0 = 0, \quad u_0 \neq 0, \quad (41)$$

and (38) simplifies to

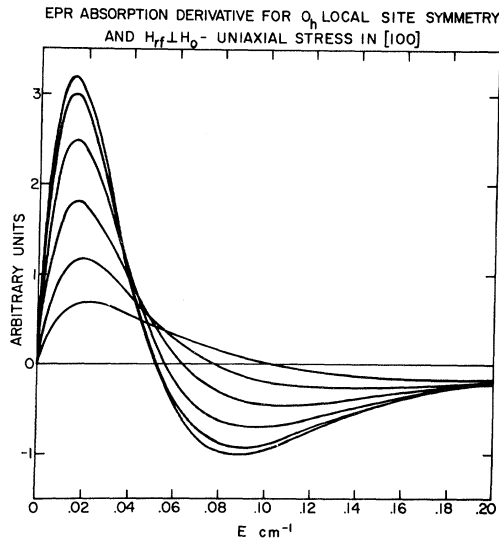


FIG. 3. EPR-absorption derivative for O_h site symmetry and $\vec{H}_{rf} \perp \vec{H}_0$ with applied stress along the [100]. The elastic constants used are those given by Huntington (see Ref. 11) for MgO, and the values for the spin-lattice coefficients are taken from an average (see Ref. 12) of those reported in the literature for MgO:Fe²⁺. The amplitude of the first lobe of the derivative decreases with increased applied stress, the values of which are successively 0, 0.1, 0.2, 0.3, 0.4, and 0.5 in units of 10^8 kg/cm². The diagonal and off-diagonal intrinsic strain parameters λ_1^{-1} and λ_2^{-1} are each taken as 1.25×10^{-4} .

$$I(E) = K e^{-(\lambda_1^2/2)u_0^2} e^{-(\lambda_2^2/4\alpha'b)E} \int_0^E d\tau [(E-\tau)^{3/2}/\tau^{1/2}] \\ \times e^{-c\tau} \cosh(\sigma\tau^{1/2}), \quad (42)$$

where

$$\sigma = \lambda_1^2 u_0 / \sqrt{\alpha'a} \quad (43)$$

and

$$c = \frac{1}{2\alpha'} \left(\frac{\lambda_1^2}{a} - \frac{\lambda_2^2}{2b} \right). \quad (44)$$

The integral in (42) is easily performed, and results in the expression

$$I(E) = K e^{-(\lambda_1^2/2)u_0^2} e^{-(\lambda_2^2/4\alpha'b)E} \sum_{n=0}^{\infty} \frac{\sigma^{2n}}{(2n)!} \\ \times \left[B\left(\frac{5}{2}, \frac{2n+1}{2}\right) E^{n+2} {}_1F_1\left(\frac{2n+1}{2}, n+3; -cE\right) \right]. \quad (45)$$

The term $B(n, m)$ in (45) is the β function¹⁰ and ${}_1F_1(p, q; z)$ is the degenerate hypergeometric series in the argument. The derivative of the absorption intensity obtained from (45) is shown in Fig. 3 for various values of the applied stress. The elastic constants used in this case are those given by Huntington¹¹ for MgO. For convenience, we set the intrinsic strain parameters λ_1 and λ_2 equal to each other and give an arbitrary value. The values for the spin-lattice coefficients G_{11} and G_{44} were taken from an average¹² of those reported in the literature for MgO:Fe²⁺.

2. Applied Uniaxial Stress along the [110]

For this condition

$$u_0 = 0, \quad r_0 \neq 0 \quad (46)$$

and (38) becomes

$$I(E) = K e^{-(\lambda_2^2/4)\alpha'b} r_0^2 e^{-(\lambda_1^2/2\alpha'a)E} \\ \times \int_0^E d\tau \frac{\tau^{3/2}}{(E-\tau)^{1/2}} e^{c\tau} e^{\sigma\tau^{1/2}}, \quad (47)$$

where

$$\rho = (\lambda_2^2/2\sqrt{\alpha'b}) r_0. \quad (48)$$

The integration in (47) is carried out to yield

$$I(E) = K e^{-(\lambda_2^2/4)\alpha'b} r_0^2 e^{-(\lambda_1^2/2\alpha'a)E} \\ \times \sum_{n=0}^{\infty} \frac{\rho^n}{n!} B\left(\frac{1}{2}, \frac{n+5}{2}\right) E^{(n+4)/2} \\ \times {}_1F_1\left(\frac{n+5}{2}, \frac{n+6}{2}; cE\right). \quad (49)$$

As in the previous case, $B(n, m)$ and ${}_1F_1(p, q; z)$ are the β function¹⁰ and the hypergeometric series in the argument, respectively. The derivative of the absorption intensity obtained from (49) is shown in Fig. 4 for various values of the applied stress. The elastic constants and intrinsic parameters are those used in Fig. 3.

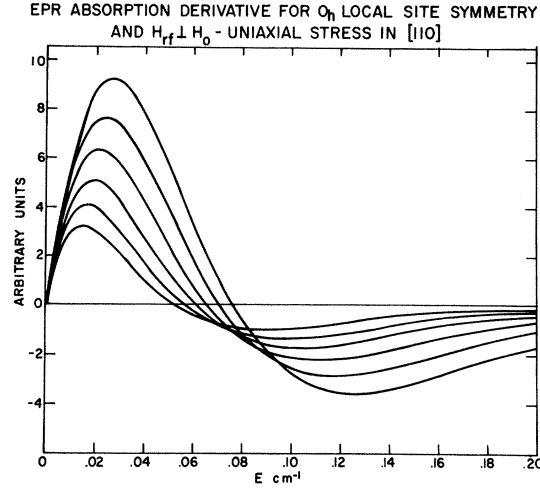


FIG. 4. EPR-absorption derivative for O_h site symmetry and $\vec{H}_{rf} \perp \vec{H}_0$ with applied stress along the [110]. The intrinsic parameters are the same as those used for Fig. 3. The first lobe of the derivative increases with applied stress, the values of which are the same as those given for Fig. 3.

Case B: $\vec{H}_{rf} \parallel \vec{H}_0$

In this case the matrix element for the rf field to first order in the spin functions is

$$|\langle i | \mathcal{H}_{rf} | f \rangle|^2 = [4 H_{rf}^2 / (h\nu_0)^2] [a(e_1 - e_2)^2 + b e_0^2]. \quad (50)$$

We let

$$\eta = \frac{2^{11/2} H_{rf}^2 \lambda_1 \lambda_2^3}{\alpha' \pi \sqrt{ab^3}} \quad (51)$$

and proceed as in case A. Then for the applied uniaxial stress along the [110], the conditions for the local induced strains are given by (46), and the expression for the absorption is

$$I(E) = \frac{1}{2} \eta e^{-(\lambda_2^2/4) r_0^2} e^{-(\lambda_1^2/2\alpha'a) E} \times \int_0^E d\tau \tau^{1/2} (E-\tau)^{1/2} e^{c\tau} e^{\rho\tau^{1/2}} \times [1 + \frac{2}{3} \tau / (E-\tau)]. \quad (52)$$

On taking the indicated integration in (52), the result is

$$I(E) = \frac{1}{2} \eta e^{-(\lambda_2^2/4) r_0^2} e^{-(\lambda_1^2/2\alpha'a) E} \sum_{n=0}^{\infty} \frac{\rho^n}{n!} E^{(n+4)/2} \times \left[B\left(\frac{3}{2}, \frac{n+3}{2}\right) {}_1F_1\left(\frac{n+3}{2}, \frac{n+6}{2}; cE\right) + \frac{2}{3} B\left(\frac{1}{2}, \frac{n+5}{2}\right) {}_1F_1\left(\frac{n+5}{2}, \frac{n+6}{2}; cE\right) \right]. \quad (53)$$

If the applied uniaxial stress is along the [100], the local induced strains obey the conditions (41).

The expression for the absorption is then

$$I(E) = \eta e^{-(\lambda_1^2/2) u_0^2} e^{-(\lambda_2^2/4\alpha'b) E} \int_0^E d\tau \tau^{1/2} (E-\tau)^{1/2} \times e^{-c\tau} \cosh(\sigma\tau^{1/2}) [1 + \frac{2}{3} (E-\tau)/\tau]. \quad (54)$$

The integral in (54) is taken to give

$$I(E) = \eta e^{-(\lambda_1^2/2) u_0^2} e^{-(\lambda_2^2/4\alpha'b) E} \sum_{n=0}^{\infty} \frac{\sigma^{2n}}{(2n)!} E^{n+2} \times \left[B\left(\frac{3}{2}, \frac{2n+3}{2}\right) {}_1F_1\left(\frac{2n+3}{2}, n+3; -cE\right) + \frac{2}{3} B\left(\frac{5}{2}, \frac{2n+1}{2}\right) {}_1F_1\left(\frac{2n+1}{2}, n+3; -cE\right) \right]. \quad (55)$$

The derivative of the absorption intensity as a function of applied stress obtained from (53) and (55) is shown in Figs. 5 and 6, respectively. The values for the elastic constants and the intrinsic parameters are the same as those used for Figs. 3 and 4.

III. DISCUSSION

From (4) and (31), the introduction of uniaxial stress shifts each homogeneous ensemble of states within the inhomogeneously broadened line to higher energy. Thus, applied stress will in general, have the effect of broadening an intrinsically strain-broadened line associated with a non-Kramers doublet. The effect for a $|\Delta M_s| = 2$ transition is therefore a broadening to lower resonance field as can be seen from Figs. 1-6.

For D_{3d} local site symmetry, (16) gives an increase in the transition probability under applied

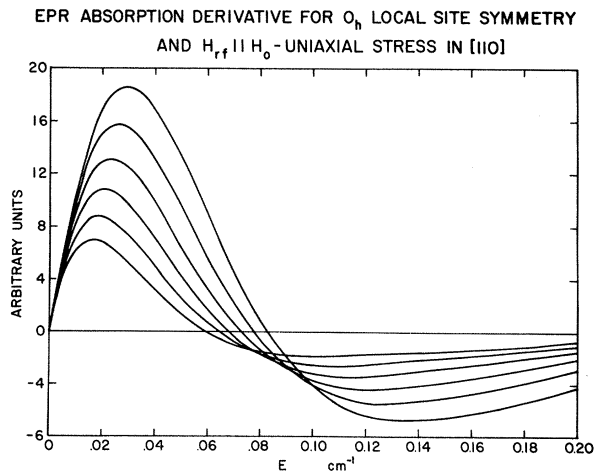


FIG. 5. EPR-absorption derivative for O_h site symmetry and $\vec{H}_{rf} \parallel \vec{H}_0$ with applied stress along the [110]. The intrinsic parameters are the same as those used for Fig. 3. The first lobe of the derivative increases with applied stress, the values of which are the same as those given for Fig. 3.

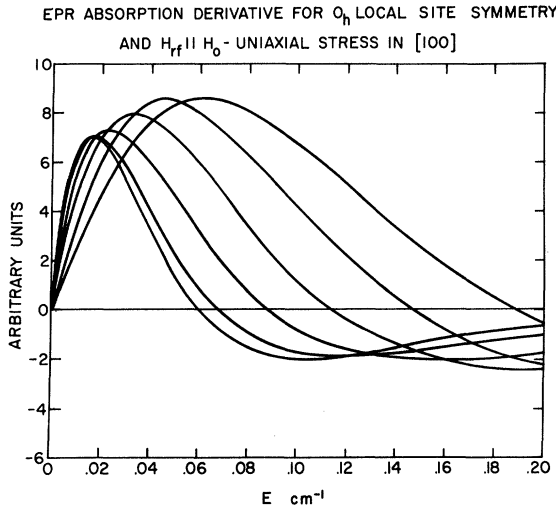


FIG. 6. EPR-absorption derivative for O_h site symmetry and $\vec{H}_{rf} \parallel \vec{H}_0$ with applied stress along the [100]. The intrinsic parameters are the same as those used for Fig. 3. The first lobe of the derivative increases with applied stress, the values of which are the same as those given in Fig. 3.

stress for each ensemble of spins, each member of which has a particular set of local strains $\{e_i\}$ giving rise to the same value for Δ . The effect is then an enhancement of the absorption intensity at each point of the resonance absorption profile which competes with the broadening due to the shift of the energy levels in the inhomogeneous distribution discussed previously. The first exponential term in (24) corresponds to the induced broadening due to the applied stress. The terms in the summation, with the exception of the first term, contribute to the enhancement of the absorption intensity which arises because of the increase in the transition probability due to applied strain. The change in the derivative of the absorption line shape is shown in Fig. 1 for various values of the applied strain. Although, the amplitude of the derivative shows a decline as the applied stress is increased, the corresponding absorption peak actually increases. The main effect is a rather large shift of the peak of the absorption to higher energy or, correspondingly, lower magnetic field.

The effect of applied strain is quite different if the local site symmetry is C_{3v} , and if the site lacks full inversion symmetry. In this case the transition probability is determined by (27), which is to first order, independent of the crystal field perturbations caused by local strains. Therefore, from (4) we expect a shift of the peak of the absorption as in the previous case, but from (27) the integrated intensity remains almost constant with applied strain. Figure 2 shows the derivative of (29) for various values of the applied strain. The same values were used

in this case for the intrinsic parameters and the applied strain as were used in the previous case. Thus, the results in Fig. 1 are contrasted with those in Fig. 2, and the discrepancies are quite marked. The main effect in this case is a spreading out of the absorption without appreciable shift in the peak until the amplitude is reduced about 80%.

For O_h local site symmetry, the same general arguments apply as were presented for the previous cases. In this case, as in the previous ones, we have considered a spin-1 formalism,^{3,6} thus the effect of the mixing of the singlet into the states of the doublet must be considered explicitly, and the effect on the shift in the resonance frequency is given by the term in Δ' in (31) where Δ' is given in terms of the crystal field perturbations by (33). We, therefore, have a dependency of the absorption intensity on the orientation of the rf magnetic field \vec{H}_{rf} with respect to the applied dc field \vec{H}_0 .

We have treated two cases: $\vec{H}_{rf} \perp \vec{H}_0$, $\vec{H}_{rf} \parallel \vec{H}_0$. In the first case, the square of the matrix element governing the transition probability is given by (36). If the uniaxial stress is applied in the [100], there is no effect on the transition probability due to the applied stress since (36) involves only shear components of the local strains.¹¹ Thus, the integrated intensity remains constant with applied stress. We expect, therefore, much the same effect as for C_{3v} symmetry shown in Fig. 2. Figure 3 shows the derivative of (45) for various values of the applied stress. It is seen that the general features are quite similar to those shown in Fig. 2.

If the applied uniaxial stress is in the [110], the transition probability will be enhanced for each spin in the system and the integrated intensity will increase. The derivative of Eq. (49) is shown in Fig. 4 for various values of the applied strain, and the intrinsic parameters and applied strains are the same as those used in Fig. 3. In this case the increase in the integrated intensity is manifest in the derivative primarily as a rather drastic increase in the area of the first lobe.

For the case in which $\vec{H}_{rf} \parallel \vec{H}_0$, the square of the matrix element which determines the transition probability is given by (50). The matrix element is sensitive to both compressive and shear components of the local strains; therefore, for applied uniaxial stress in either the [110] or the [100] the integrated intensity will increase as stress is applied. For the former case, the derivative of (53) is shown in Fig. 5, and for the latter case the derivative of (55) is shown in Fig. 6.

From (6) through (8), (34), (36) and (50), it is evident that the compressive strain components perpendicular to the axis of quantization enter the expressions entirely as the difference of one another, and that the strain component along the axis of quantization does not appear in any of the expressions.

Thus, only local crystal field perturbations which lower the symmetry will have an effect on the separation between the levels of the doublet and/or the transition probability. In other words, hydrostatic pressure will have no effect on the line shape to second order. Thus, small perturbations on the local crystal field symmetry are directly manifest in terms of the effects on the absorption line shape.

IV. CONCLUSION

The model presented here offers a means for studying the effect of intrinsic and induced perturbations on the local crystal field symmetry for transitions within a non-Kramers doublet for the three cases of local crystal-field symmetry considered.

Using uniaxial stress, the spin-lattice coupling parameters can be evaluated independently of the concentration of the impurity ion to the extent that the impurity concentration is not so large as to affect the shape of the absorption line.

The model is applicable to a variety of systems, among them are MgO: Fe^{2+} ,¹² $\text{Al}_2\text{O}_3: \text{Fe}^{2+}$,⁹ and $\text{CaF}_2: \text{U}^{4+}$.^{13,14} For the latter system, the model has been compared quite favorably with the results of uniaxial strain measurements.¹⁴

ACKNOWLEDGMENTS

The authors wish to express thanks to J. D. Stettler and E. R. Wilkinson of this Laboratory for useful discussions.

¹G. Watkins and E. R. Feher, Bull. Am. Phys. Soc. **7**, 29 (1962).

²E. R. Feher, Phys. Rev. **136**, 145 (1964).

³C. M. Bowden, H. C. Meyer, and P. L. Donoho, Inter. J. Quantum Chem. Suppl. **3**, 617 (1970).

^{3a}Note added in proof. The term doublet is used here to denote the $|\Delta M_s| = 2$ transition within a ground triplet.

⁴J. W. Culvahouse, D. P. Schinke, and D. L. Foster, Phys. Rev. Letters **18**, 117 (1967).

⁵C. M. Bowden, H. C. Meyer, and P. L. Donoho, preceding paper, Phys. Rev. B **3**, xxx (1971).

⁶K. A. Mueller, Phys. Rev. **171**, 350 (1968).

⁷W. Voigt, *Lehrbuch der Kristallphysik* (Teubner, Leipzig, 1910).

⁸N. Bloembergen, Science **133**, 1363 (1961).

⁹C. M. Bowden, H. C. Meyer, and P. L. Donoho, Inter. J. Quantum Chem. Suppl. **4**, 1971 (1970).

¹⁰J. S. Gradshteyn and I. M. Ryzhik, *Table of Integrals, Series and Products* (Academic, New York, 1965).

¹¹H. B. Huntington, *Solid State Physics* (Academic, New York, 1958), Vol. 7, p. 276.

¹²D. H. McMahon, Phys. Rev. **134A**, 128 (1964).

¹³P. K. Wunsch, P. L. Donoho, H. C. Meyer, and C. M. Bowden, Bull. Am. Phys. Soc. **15**, 250 (1970).

¹⁴P. L. Donoho, P. K. Wunsch, P. F. McDonald, C. M. Bowden, and H. C. Meyer, Bull. Am. Phys. Soc. **15**, 250 (1970).

Conduction-Electron Spin Resonance in a Lithium Film*

Joe H. Pifer and Richard Magno

Rutgers University, New Brunswick, New Jersey 08903

(Received 2 October 1969)

The use of a linear resonator instead of a microwave resonant cavity increases the sensitivity of any resonance spectrometer when studying electron resonance in metals. This technique is used to study the temperature dependence of the line shape of the conduction-electron spin resonance in a lithium film for thicknesses ranging from 0.3 to 30 skin depths. Dyson's theory is found to apply at high temperatures. Deviations below 120 °K due to the anomalous skin effect provide a method of determining the microwave surface impedance in the alkali metals.

I. INTRODUCTION

In this paper we discuss a simple modification of the conventional electron-spin-resonance (ESR) technique for metals, which results in a sensitivity gain of five times. We then use this technique to verify Dyson's¹ theory of the conduction-electron spin resonance (CESR) line shape in lithium films whose thicknesses range from 0.3 to 30 skin depths. Dyson's theory has previously been verified² for

thick samples and for dispersions or powders whose grain size is small compared to the skin depth. Here we study a *single* film of uniform thickness. Data were taken from 4.2 °K to room temperature. At low temperatures, the anomalous skin effect is found to modify the line shape in an extremely simple manner.

The usual reflection technique for studying CESR in metals is to place the sample in a cavity which is critically coupled to one arm of a microwave bridge.